ARTICLE
Journal of Cellular Biochemistry 116:2018–2031 (2015)

Journal of Cellular Biochemistry

Systems Chemo-Biology and Transcriptomic Meta-Analysis Reveal the Molecular Roles of Bioactive Lipids in Cardiomyocyte Differentiation

Joice de Faria Poloni and Diego Bonatto*

Centro de Biotecnologia da Universidade Federal do Rio Grande do Sul, Departamento de Biologia Molecular e Biotecnologia, Universidade Federal do Rio Grande do Sul, Porto Alegre, RS, Brazil

ABSTRACT

Lipids, which are essential constituents of biological membranes, play structural and functional roles in the cell. In recent years, certain lipids have been identified as regulatory signaling molecules and have been termed "bioactive lipids". Subsequently, the importance of bioactive lipids in stem cell differentiation and cardiogenesis has gained increasing recognition. Therefore, the aim of this study was to identify the biological processes underlying murine cardiac differentiation and the mechanisms by which bioactive lipids affect these processes. For this purpose, a transcriptomic meta-analysis of microarray and RNA-seq data from murine stem cells undergoing cardiogenic differentiation was performed. The differentially expressed genes identified via this meta-analysis, as well as bioactive lipids, were evaluated using systems chemo-biology tools. These data indicated that bioactive lipids are associated with the regulation of cell motility, cell adhesion, cytoskeletal rearrangement, and gene expression. Moreover, bioactive lipids integrate the signaling pathways involved in cell migration, the secretion and remodeling of extracellular matrix components, and the establishment of the cardiac phenotype. In conclusion, this study provides new insights into the contribution of bioactive lipids to the induction of cellular responses to various stimuli, which may originate from the extracellular environment and morphogens, and the manner in which this contribution directly affects murine heart morphogenesis. J. Cell. Biochem. 116: 2018–2031, 2015.

KEY WORDS: EXTRACELLULAR ENVIRONMENT; CARDIOMYOCYTE DIFFERENTIATION; CELL SIGNALING; MICROARRAY; RNA-SEQ

Bioactive lipids are known to act both as structural components in cellular membranes and as signaling and regulatory molecules under a wide range of physiological and pathological conditions [Wang et al., 2006; Hannun and Obeid, 2008; Berdichevets et al., 2010]. The best-studied bioactive lipids are sphingosine (Sph), ceramide (Cer), sphingosine-1-phosphate (S1P), sphingomyelin (SM), lysophosphatidic acid (LPA), and phosphatidic acid (PA). These molecules participate in essential cellular functions such as differentiation, proliferation, survival and apoptosis, migration, polarity, and cytoskeletal regulation [Wang et al., 2006; Hannun and Obeid, 2008; Berdichevets et al., 2010; Kleger et al., 2011; de Faria Poloni et al., 2014]. Bioactive lipids act as cell signaling molecules via (a) direct interactions with specific protein partners, (b) lipid rafts, which influence cell-signaling cascades, and (c) interactions with other lipids, which affect the cell membrane structure or the interaction landscape between proteins and the membrane [Hannun and Obeid, 2008; Bieberich 2012].

Studies have demonstrated the activity of bioactive lipids in cardiomyocyte differentiation and survival [Kupperman et al., 2000; Karliner et al., 2001; Wendler and Rivkees, 2006; Kleger et al., 2011;

Abbreviations: Cer, ceramide; CP, cardiac precursor; CMs, cardiomyocytes; DEG, differentially expressed gene; ECM, extracellular matrix; HB, hub-bottleneck; LPA, lysophosphatidic acid; PA, phosphatidic acid; PE, phosphorylethanolamine; PtdC, phosphatidylcholine; PtdG, phosphatidylglycerol; PtdI, phosphatidylinositol; PtdS, phosphatidylserine; S1P, sphingosine-1-phosphate; SM, sphingomyelin; SPC, sphingosylphosphorylcholine; Sph, sphingosine.

Conflict of interest: The authors have declared no conflict of interest.

Grant sponsor: CNPq; Grant number: 301149/2012-7; Grant sponsor: CAPES; Grant number: 004/12; Grant sponsor: FAPERGS; Grant number: 11/2072-2.

*Correspondence to: Diego Bonatto, Centro de Biotecnologia da UFRGS – Sala 219, Departamento de Biologia Molecular e Biotecnologia, Universidade Federal do Rio Grande do Sul – UFRGS, Avenida Bento Gonçalves 9500 – Prédio 43421, Postal Code 15005, Porto Alegre – Rio Grande do Sul, Brazil.
E-mail: diegobonatto@gmail.com,diego@cbiot.ufrgs.br

Manuscript Received: 1 March 2015; Manuscript Accepted: 3 March 2015

Accepted manuscript online in Wiley Online Library (wileyonlinelibrary.com): 9 March 2015

DOI 10.1002/jcb.25156 • © 2015 Wiley Periodicals, Inc.

de Faria Poloni et al., 2014]. Additionally, bioactive lipid-associated metabolic alterations disturb cardiac contractility and induce abnormal development in terms of heart structure morphology and vascular maturation [Xu et al., 1996; de Faria Poloni et al., 2014]. Unfortunately, the molecular pathways through which bioactive lipids influence heart development are currently poorly understood.

The aim of this study was to investigate the genes related to bioactive lipid signaling during cardiac differentiation, using *Mus musculus* as a model organism. For this purpose, a transcriptomics meta-analysis and systems chemo-biology analyses were performed. Additional data gathered from network clustering and gene ontology (GO) analyses associated with the evaluation of the local network topologies (centralities) indicated that bioactive lipids influence cardiac morphogenesis by modulating signaling pathways that promote cytoskeletal reorganization, extracellular matrix (ECM) remodeling and cell communication regulation. Furthermore, interference analysis, which enables the determination of the effect of a small molecule and/or macromolecule on the network, was performed on selected bioactive lipids using a virtual knockout model. For this purpose, molecules that potentially mediate the interplay between extracellular stimuli and cellular responses were obtained. This study provides new evidence for the significance of bioactive lipids in differentiation and the regulation of heart development.

MATERIALS AND METHODS

GENE EXPRESSION DATA FROM THE MYOCARDIAL DIFFERENTIATION OF STEM CELLS

The transcriptomic profile of myocardial differentiation was obtained from the Gene Expression Omnibus (GEO) database [http://www.ncbi.nlm.nih.gov/geo]. For this purpose, the gene expression of *Mus musculus* was profiled via microarray and RNA-seq analysis of the matrix files GSE6689 and GSE47948, respectively [Faustino et al., 2008; Wamstad et al., 2013].

The matrix file GSE6689 represents a gene expression analysis performed on murine embryonic stem cells (ESCs) that were cultured and subjected to cardiogenesis, as reported by Faustino et al. in 2008 [Faustino et al., 2008]. The microarray series matrix file (GSE6689) and its platform (GPL1261) were downloaded from [ftp://ftp.ncbi.nlm.nih.gov/geo/series/GSE6nnn/GSE6689/matrix/] and [http://www.ncbi.nlm.nih.gov/geo/query/acc.cgi?acc=GPL1261], respectively. Microarray analysis was performed by considering undifferentiated ESCs as the control group and cardiac precursor (CP) cells and cardiomyocytes (CMs) as the experimental groups, after which the differentially expressed gene (DEGs) were identified (Fig. 1). The DEGs identified based on microarray analysis were evaluated using R statistical programming language tools and the Bioconductor package Linear Models for Microarray Data (limma; Fig. 1) [Smyth, 2005].

Additionally, the transcriptomic data from matrix file GSE47948, in which murine ESCs were cultured and underwent cardiogenesis, as reported by Wamstad et al. in 2013, were used [Wamstad et al., 2012]. The DEGs from the RNA-seq data were analyzed by considering the ESCs as the control group, which was compared to CP cells and CMs using the R statistical programming language (Fig. 1). For this purpose, FastQC was used to evaluate the read quality [Patel and Jain, 2012]. This step was followed by read alignment using the most recent reference genome and the gene annotations for *Mus musculus* [available at http://www.ensembl.org/info/data/ftp/index.html] using Bowtie2 2.1 [Langmead and Salzberg, 2012]. Splice junctions were identified using TopHat2 2.0.11 [Trapnell et al., 2012]. Read counts were performed using HTSeq 0.6.1, and DEGs were identified via analysis using edgeR [Robinson et al., 2010; Anders et al., 2014]. For both transcriptomes (GSE6689 and GSE47948), $\log_2$FC >2.0 and a false discovery rate (FDR) threshold of < 0.05 (Fig. 1) were used as criteria to generate the DEG list.

DATA MINING AND INTERACTOMIC NETWORK DESIGN

To evaluate the association between lipids and cardiomyocyte differentiation, interactomic data mining was performed. For this purpose, the obtained DEGs were used as input data for the metasearch engine STRING 9.1 [Franceschini et al., 2013]. The following parameters were used in the STITCH program: all prediction methods enabled, excluding text mining, and a degree of confidence of 0.400. The resulting interactomic data were further analyzed using Cytoscape 2.8.3 [Smoot et al., 2011; Cline et al., 2007] (Fig. 1), resulting in the generation of two major networks: (i) the CP network, which represents the node-DEGs from comparisons between CPs cells and ESCs, and (ii) the CM network, which represents the node-DEGs from comparisons between CMs and ESCs (Supp. 1A and B). The most commonly reported bioactive lipids in the literature (Sph, Cer, S1P, SM, LPA, and PA) were used as input data for STITCH 3.1 to design the network related to bioactive lipids signaling, using the same parameters described for STRING 9.1 (Fig. 1) [Kuhn et al., 2012]. The bioactive lipid interactomic data obtained from STITCH 3.1 were merged with both the CP and CM networks in Cytoscape 2.8.3.

Furthermore, the nodes within both networks were colored according to the $\log_2$FC values of the DEGs. Thus, the light blue nodes represent genes with decreased expression based on either the microarray or RNA-seq analysis, whereas the dark blue nodes represent genes with decreased expression based on both the microarray and RNA-seq analyses (Supp. 1A and B). Furthermore, those gene nodes displaying increased expression were characterized by an orange color when these nodes were identified based on either the microarray or RNA-seq analysis, whereas red nodes denote genes detected based on both the microarray and RNA-seq analyses (Supp. 1A and B). To visualize the number of overexpressed and underexpressed genes shared and exclusive of the CP and CM networks, different Venn Diagrams were created using the online tool Data Overlapping and Area-Proportional Venn Diagram [http://apps.bioinforx.com/bxaf6/tools/app_overlap.php].

Moreover, the LIPID MAPS, KEGG, and AmiGO 1.8 search engines were used according to their default parameters as additional data mining tools [Kanehisa and Goto, 2000; Fahy et al., 2007; Carbon et al., 2009].

CLUSTER ANALYSIS OF THE INTERATOMIC NETWORK

The composition of the major clusters in the main network was analyzed using the program Allegro Molecular Complex Detection

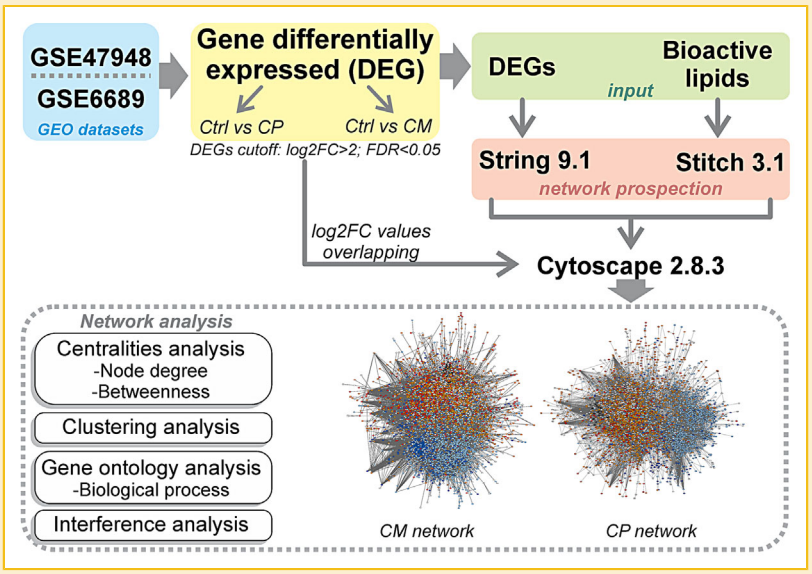

Fig. 1. Systems chemo-biology analysis workflow. The transcriptomic datasets (GSE47948 and GSE6689) were obtained and evaluated for DEGs from distinct stages (CP cells and CMs) using the following thresholds: $\log_2FC > 2$ and FDR < 0.05. DEGs and bioactive lipids were used as the inputs into STRING 9.1 and STITCH 3.1, respectively. Two interatomic networks were designed from the CP and CM networks data and were visualized using the Cytoscape 2.8.3 program. The $\log_2FC$ values were overlaid onto the networks. Centrality analysis was performed to evaluate the node degree and betweenness parameters. The networks were also subjected to clustering and GO analyses to identify the most relevant biological processes. Finally, interference analysis was used to perform virtual knockouts of the HB bioactive lipids.

(AllegroMCODE) according to the following pre-processing parameters: degree threshold, 2; node score threshold, 0.2; k-core, 2; and maximum network depth, 100 (Fig. 1) [Bader and Hogue, 2003). The following post-processing parameters were used: expansion of a cluster by one neighbor shell allowed (fluff option enabled) using a node density threshold of 0.1 and deletion of a single connected node from clusters (haircut option enabled). Thus, each cluster displayed a degree of connection for a given group of nodes, also referred to as the "cliquishness" (C*i*) value. In this study, C*i* > 3.5 was used as the threshold.

GO ANALYSIS

The major biological processes, molecular functions, and cellular components associated with each cluster and gene set for the genes displaying decreased and increased expression were determined using the plugin Biological Network Gene Ontology (BiNGO) 2.44, a Cytoscape 2.8.3 plugin (Fig. 1) [Maere et al., 2005]. The degree of functional enrichment for a given GO category was quantitatively assessed (*P*-value) based on a hypergeometric distribution [Rivals et al., 2007]. A correction for multiple comparisons was performed by applying the FDR algorithm, which was fully implemented in the BiNGO software, at a significance level of adjusted $P < 0.05$ [Benjamini and Hochberg, 1995]. In addition, the most representative biological processes, molecular functions, and cellular components in each cluster were selected and classified according to their gene expression (increased or decreased) and the experiment that provided these gene expression data (microarray, RNA-Seq, or both).

CENTRALITY ANALYSIS

Centrality analysis was performed using the Centiscape 1.21 software [Scardoni et al., 2009]. This analysis evaluated the most relevant nodes in the network according to the following selected centrality parameters: node degree and betweenness (Fig. 1). Betweenness analysis involved calculating the shortest paths connecting adjacent nodes that pass through each node, as reported by Scardoni and Laudanna [2012]. Additionally, node degree analysis involved evaluating nodal connectivity, which was expressed as the number of connections for a given node Scardoni and Laudanna [2012]. An average score was calculated for the node degree and the betweenness using the following definitions: hub, a node with a higher node degree score than that of the network average; bottleneck, a node with a higher betweenness score than that of the network average [Newman, 2005; Scardoni and Laudanna, 2012]. Therefore, nodes whose betweenness and node degree were higher than the network values were defined as hub-bottleneck (HBs). HBs may perform key regulatory functions in the cell; they are also likely to be associated with different clusters or biological processes [Newman, 2005; Scardoni and Laudanna, 2012]. Furthermore, the number of overexpressed and underexpressed HB genes shared and exclusive of the CP and CM networks were visualized with different Venn Diagrams using the online tool Data Overlapping and Area-Proportional Venn Diagram [http://apps.bioinforx.com/bxaf6/tools/app_overlap.php].

INTERFERENCE ANALYSIS

Interference 1.0 is a Cytoscape software plug-in that can be used to evaluate the functional influence of a single node or multiple nodes on the network topology via a virtual knockout experiment [Feltes and Bonatto, 2013; Scardoni et al., 2014]. For this evaluation, the betweenness parameter was selected to be recomputed on the network after each node was removed. Each node represented by an

HB bioactive lipid in the CP and CM networks was removed to evaluate its effect on the betweenness of each remaining node. In this sense, interference analysis was performed for each cluster that contained bioactive lipids (clusters I-CP, II-CP, III-CP, and III-CM).

Interference analysis can determine whether removing a given node or multiple nodes positively or negatively affects the betweenness score. Negative interference indicates that the removal of a given node increases the centrality value of a target node, meaning that the presence of a given node is disadvantageous to the topology of the target node. In contrast, positive interference indicates that the removal of a given node disrupts the topology of the target nodes. To obtain our results, we focused on nodes that induced the highest positive and the lowest negative interference on their target nodes.

RESULTS

NETWORK DESIGN AND TRANSCRIPTOMIC META-ANALYSIS OF CARDIAC PRECURSOR (CP) CELLS AND CARDIOMYOCYTES (CMS)

Our transcriptomic and interatomic analyses revealed two networks displaying distinct transcriptomic profiles: the CP and CM networks (Fig. 1 and Supp. 1). The CP network contains DEGs identified based on comparisons between CP cells and ESCs, and the CM network contains DEGs identified based on comparisons between CMs and ESCs. The CP network was composed of 3,921 nodes and 18,514 edges (Supp. 1A), whereas the CM network was composed of 4,906 nodes and 24,728 edges (Supp. 1B).

Network examination in STITCH 3.1, using bioactive lipids as an input, allowed us to obtain 19 lipids and their derivatives, such as Sph, S1P, Cer, SM, sphingosylphosphorylcholine (SPC), phosphorylethanolamine (PE), phosphatidylinositol (PtdI), phosphatidylglycerol (PtdG), phosphatidylcholine (PtdC), phosphatidylserine (PtdS), PA, and LPA. These small molecules are shared in the CP and CM networks and shown as black nodes (Supp. 1A and B).

The DEG data obtained from the microarray or RNA-seq meta-analysis or both were overlaid onto the CP and CM networks (Fig. 1 and Supp. 1), generating the "node-DEGs", a multiplex representation of genes. In this representation, the CP network is composed of 1,613 overexpressed genes and 1,395 underexpressed genes (Supp. 1A), whereas the CM network is composed of 2,042 overexpressed genes and 2,009 underexpressed genes (Supp. 1B). Furthermore, we evaluated the number of shared and non-shared node-DEGs between the CP and CM networks (Fig. 2A and B), revealing that 1,278 overexpressed node-DEGs and 1,248 underexpressed node-DEGs were shared between the CP and CM networks (Fig. 2A and B). However, the CP network contained 335 overexpressed genes and 147 underexpressed genes that were not shared, whereas the CM network contained 764 overexpressed genes and 761 underexpressed genes that were not shared (Fig. 2A and B).

The associated node-DEGs from the shared and non-shared groups were selected for GO analysis (Fig. 2A and B). The resulting overexpressed node-DEGs that were shared between the CP and CM networks were overrepresented by sphingolipid and membrane lipid metabolic processes, heart and mesoderm morphogenesis, cytoskeleton and ECM organization, and cardiac muscle tissue development (Fig. 2A). Interestingly, the underexpressed node-DEGs that were shared between the CP and CM networks were overrepresented by biological processes associated with the regulation of cell proliferation, chromatin modification, and DNA repair (Fig. 2B).

Various node-DEGs that encode proteins associated with bioactive lipid metabolism and signaling were found to be overexpressed node-DEGs that were shared between the CP and CM networks (Table I). Furthermore, bioactive lipids interact with several overexpressed node-DEGs whose expression is essential for cell signaling. Moreover, S1P appeared in the both CP and CM networks to be associated with Akt1, Fn1, IL6, Nos3, Rac1, Rhoa, and Vegfa (Fig. 3A and B). Additionally, LPA was directly associated with Akt1, Edn1, Fn1, Ptk2, Pxn, Rac1, Rhoa, Rhod, and Src (Fig. 3A and B).

CENTRALITY AND GO ANALYSES

Centrality analysis indicated that the HBs-associated subnetwork from the CM and CP networks was composed of 534 nodes and 5,333 edges in the CP network, and 650 nodes and 7,676 edges in the CM network (Supp. 1A and B). These HB nodes are represented in the networks with a thick edge. Small molecules, such as Cer, LPA, PA, Sph, and S1P, were also found to be HB nodes (Supp. 1A and B). In addition, various HBs that are associated with bioactive lipids, such as Cav1, LPAR, Sphk1, and Smpd1, were detected (Supp. 1 and Fig. 3). Moreover, we detected several overexpressed HB node-DEGs related to the ECM, cell adhesion, and integrin signaling in the CM and CP networks; these genes included Col1a1, Col1a2, Col3a1, Col6a2, Lama2, Mmp2, Cyr61, Itga4, Itga5, Itga7, Itgb1, Fn1, Pxn, Msn, Actb, and Actn1 (Supp. 1).

Several HBs that were overexpressed node-DEGs associated with murine heart development were found, such as Tbx2, Tbx5, Hand2, Bmp2, Bmp4, Bmp7, Isl1, TGF- β1, Gata4, Gata6, Nkx2-5, and Erbb2 (Supp. 1).

We also evaluated shared and non-shared overexpressed and underexpressed node-DEGs in HB subnetworks from the CP and CM networks, followed by GO analysis (Fig. 4A and B). This analysis revealed that the shared overexpressed HB node-DEGs were associated with cell communication, heart morphogenesis, cytoskeletal organization, cell–cell and cell–matrix adhesion, ECM organization, integrin-mediated signaling, positive regulation of lipid kinase activity, and positive regulation of lipid metabolic processes (Fig. 4A). Alternatively, the underexpressed node-DEGs shared between the CP and CM networks were represented by DNA replication and the cell cycle (Fig. 4B).

CLUSTERING AND GO ANALYSIS

Clustering analysis of the networks was performed to understand the role of bioactive lipids in cardiac differentiation. Clusters above the threshold values containing similar GO were merged, resulting in four major clusters identified in both the CP and CM networks (Supp. 2). The predominant biological processes observed in clusters I-CP, II-CP, and III-CP were heart morphogenesis, migration, cell adhesion, and ECM organization (Supp. 3A–C). Nevertheless, cell differentiation, tissue remodeling, and regulation of heart contraction were present in I-CP and II-CP (Supp. 3A and B). In addition, regulation of programmed cell death and apoptosis are observed in CI-CP, CIII-CP, and CIII-CM (Supp. 3A, C and 4C). Biological processes related to the response to lipids, cellular membrane

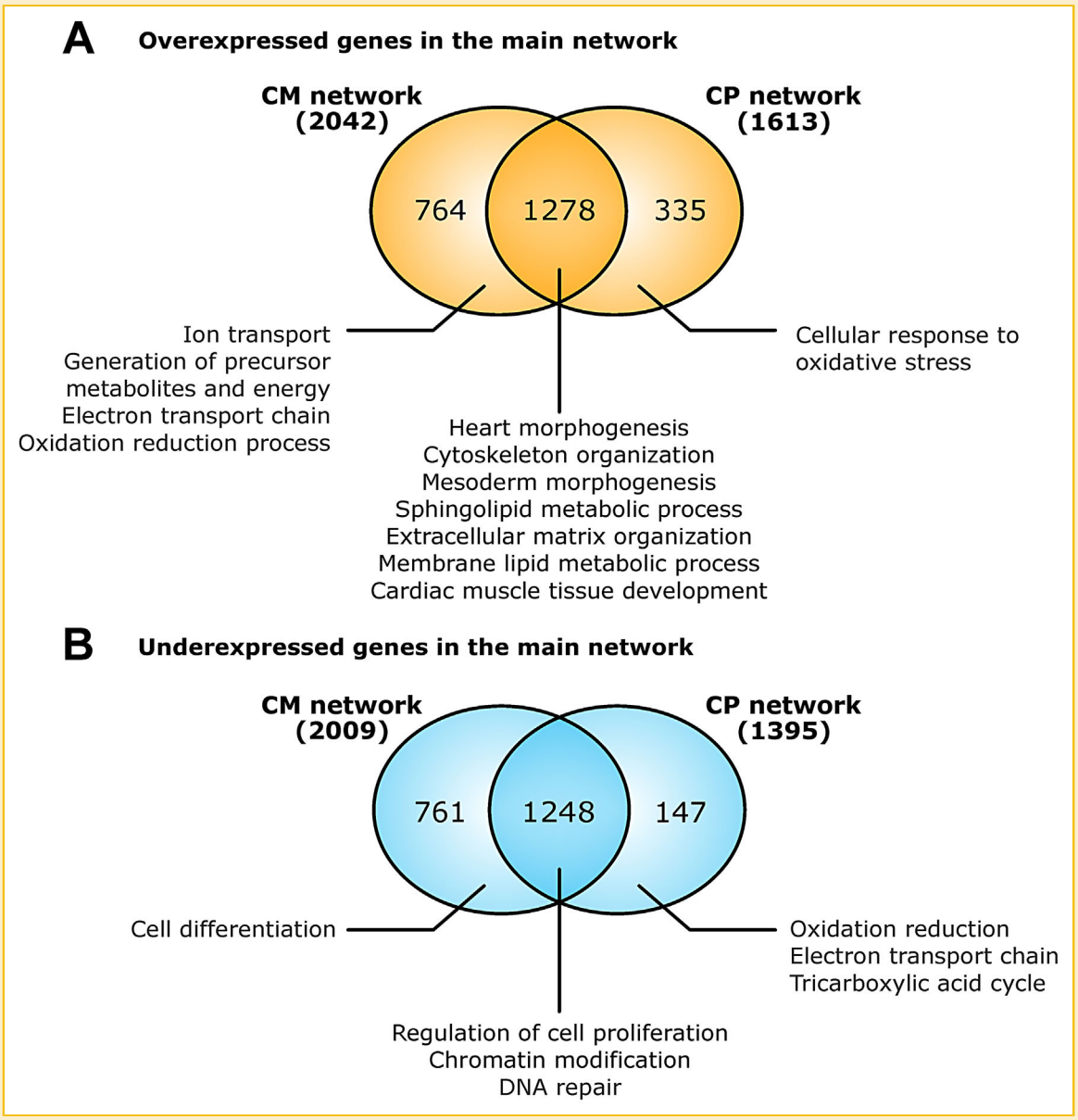

Fig. 2. (A) Comparative GO analysis of all of the overexpressed node-DEGs in the CM and CP networks. (B) Comparative GO analysis of all of the underexpressed node-DEGs in the CM and CP networks.

organization, and lipid and sphingoid metabolism were also represented in clusters I-CP, II-CP, and III-CP, which may indicate a relationship between bioactive lipids and morphogenetic processes (Supp. 3A–C). Additionally, the majority of the node-DEGs that encode proteins related to these processes were overexpressed (Supp. 3A–C). Interestingly, in these CP clusters, cellular component analysis indicated several overexpressed genes related to cytoskeleton, membrane raft, plasma membrane, and ECM (Supp. 3A–C). Additionally, the prevalent molecular functions among I-CP, II-CP, and III-CP were transferase activity, ECM structural constituent, transmembrane receptor protein kinase activity, and ultimately lipid binding observed in II-CP and III-CP (Supp. 3B and C). Nonetheless, Rho guanine-nucleotide exchange factor, ceramidase, and bioactive lipid receptor activity were observed in III-CP (Supp. 3C).

In the CM network, the biological processes of heart development and morphogenesis, migration, ECM organization, tissue remodeling, and cytoskeleton organization were detected in clusters I-CM and III-CM, which were predominantly represented by overexpressed node-DEGs (Supp. 4A and C). Furthermore, molecular function analysis of III-CM showed sphingolipid binding, bioactive lipid receptor activity, ceramidase, and sphingomyelin phosphodiesterase activity, and extracellular matrix structural constituent, in addition to collagen, laminin, and fibronectin binding (Supp. 4A and C). According to cellular component analysis of I-CM and III-CM, the prevalent results

TABLE I. Overexpressed Node-DEGs Shared Between the CP and CM Networks and Associated With Bioactive Lipid Metabolism

Gene	Description	Function
Agpat-1, -3, -6, -9	Lysophosphatidic acid acyltransferase	Converts lysophosphatidic acid to phosphatidic acid
Asah-1, -2	N-acylsphingosine amidohydrolase	Hydrolyzes ceramide into sphingosine
Cerk	Ceramide kinase	Promotes the phosphorylation of ceramide, generating ceramide-1-phosphate
Lass4	(Dihydro) ceramide synthase	Involved in the ceramide de novo synthesis pathway, which converts dihydrosphingosine to dihydroceramide
Lpar-1, -3	Lysophosphatidic acid receptor	Membrane receptor of lysophosphatidic acid
Pld-1, -2	Phospholipase D2	Catalyzes the conversion of phosphatidylcholine to phosphatidic acid
Ppap-2a, -2b	Phosphatidic acid phosphatase type 2	Catalyzes the conversion of phosphatidic acid to diacylglycerol
S1pr-1, -3	Sphingosine-1-phosphate receptor	Membrane receptor of sphingosine-1- phosphate
Sgpl1	Sphingosine phosphate lyase	Promotes the cleavage of phosphorylated sphingoid bases
Sgpp1	Sphingosine-1-phosphate phosphatase	Catalyzes sphingosine-1-phosphate degradation via salvage and promotes the recycling of sphingosine
Smpd-1, -3	Sphingomyelinase	Converts sphingomyelin to ceramide
Sphk1	Sphingosine kinase	Promotes the phosphorylation of sphingosine, generating sphingosine-1-phosphate
Spns2	Spinster homolog 2	Mediates sphingosine-1-phosphate cell export
Sptlc1	Serine palmitoyltransferase	Converts L-serine and palmitoyl-CoA to 3-ketodihydrosphingosine. Promotes the first step of the de novo biosynthesis of ceramide

were membrane raft, cytoskeleton, and extracellular space (Supp. 4A and C). Alternatively, cluster II-CM was related to cardiac metabolism associated with heart contraction, including contractile fiber, sarcomere, and cytoskeleton as the prevailing cellular components, while molecular function is dictated by structural constituent of cytoskeleton and motor activity (Supp. 4B).

Clusters IV-CP and IV-CM were primarily represented by under-expressed node-DEGs related to the cell cycle, RNA processing, DNA repair, and replication, and are shown as the major cellular component chromosome, heterochromatin, and nuclear lumen (Supp. 3D and 4D).

INTERFERENCE ANALYSIS

The most relevant results according to the interference analysis were selected within each analyzed cluster and are presented in Table II. Virtual knockout of the HB bioactive lipids (S1P, Cer, Sph, PA, LPA) interfered with the betweenness score of several nodes related to cardiac development, indicating that in a biological context, these target nodes can be regulated by the removed nodes. According to our results, the virtual knockout of S1P positively interfered with Vegfa, Nos3, Il6, Ptgs2, Rhoa, and the chemokines Cxcl12, Cxcl13, and Cxcr4, reducing their topological importance in the network (Table II). However, S1P could not be evaluated in CIII-CP and CIII-CM due the network fragmentation, which rendered the calculations impossible. Furthermore, LPA affected the betweenness score of Src, Egfr, Pxn, Edn1, Ptk2, and the Rho GTPases Rhoa and Rhod, indicating a role for LPA in maintaining the topology of these nodes (Table II). The main targets that were positively affected by virtual knockout of Cer were Hand2, Edn1, Cd44, Casp8, Serpine1, Ptgs2, Bcl2l1, Fas, and Il6, while the negatively affected nodes were Nos3, Mmp2, and Mmp9 (Table II). In addition, PA improve the betweenness score of Mmp9, while Sph negatively interfered with Egfr, Cxcl12, Cxcr4, and Src in CIII-CP (Table II).

DISCUSSION

MEMBRANE DYNAMICS

The embryonic vertebrate heart undergoes a series of orchestrated events during cardiac development, growth, and maturation; these events involve cell movements and morphological transformations [Chen et al., 2005]. The ECM is a dynamic structure that provides a scaffold for cell adhesion in the interstitial space and that also facilitates the propagation of mechanical signals [Little and Rongish, 1995; Bowers et al., 2010; Rozario and Desimone, 2010]. During cardiac development, different stimuli, such as rhythmic contractions that start early in cardiomyocytes and cytokines produced by cardiac myofibroblasts, are able to influence heart remodeling [Porter and Turner, 2009; Wozniak and Chen, 2009; Granados-Riveron and Brook, 2012]. These stimuli can transiently activate plasma membrane SMases, an overexpressed HB in the CP and CM networks (Fig. 3) whose activity (sphingomyelin phosphodiesterase) was detected by GO analysis in III-CM (Supp. 4C), and promote Cer and PtdC production (Fig. 5A) [Czarny and Schnitzer, 2004]. Moreover, SM cleavage promotes the redistribution of cholesterol in the plasma membrane bilayer, altering the cholesterol concentration and modulating the activity of membrane-associated signal transduction proteins (Fig. 5A) [Armstrong and Zidovetzki, 2008; Qin et al., 2012]. Accordingly, GO analysis indicated the membrane lipid metabolic process represented by overexpressed node-DEGs in the main network and in the III-CP cluster, which also showed cellular membrane organization, mostly represented by overexpressed genes (Fig. 2A and Supp. 3C). In addition, membrane rafts and caveolae were associated with I-CP, III-CP, and III-CM (Supp. 3A, C and 4C). Interestingly, Groenendijk et al. [2007] published a review that emphasized the important role of shear stress in providing a mechanical stress necessary for normal heart development and in affecting the expression of genes, such as Edn1 and Nos3, that will be discussed later as the targets of bioactive lipids.

CELL MOTILITY, MIGRATION, AND CYTOSKELETAL REORGANIZATION

Transient increases in Cer levels promote the activation of a signaling cascades triggered by Src (Fig. 5B) [Czarny and Schnitzer, 2004]. The Src-associated node-DEG was overexpressed in the CP and CM networks and was also associated with bioactive lipids, in addition to being topologically affected by LPA virtual knockout (Fig. 3 and Table II). LPA also negatively affected Ptk2 and Pxn topology in CIII-CP (Table II). Src regulates Cav1 cellular localization and mediates Ptk2 phosphorylation, modulating F-actin dynamics,

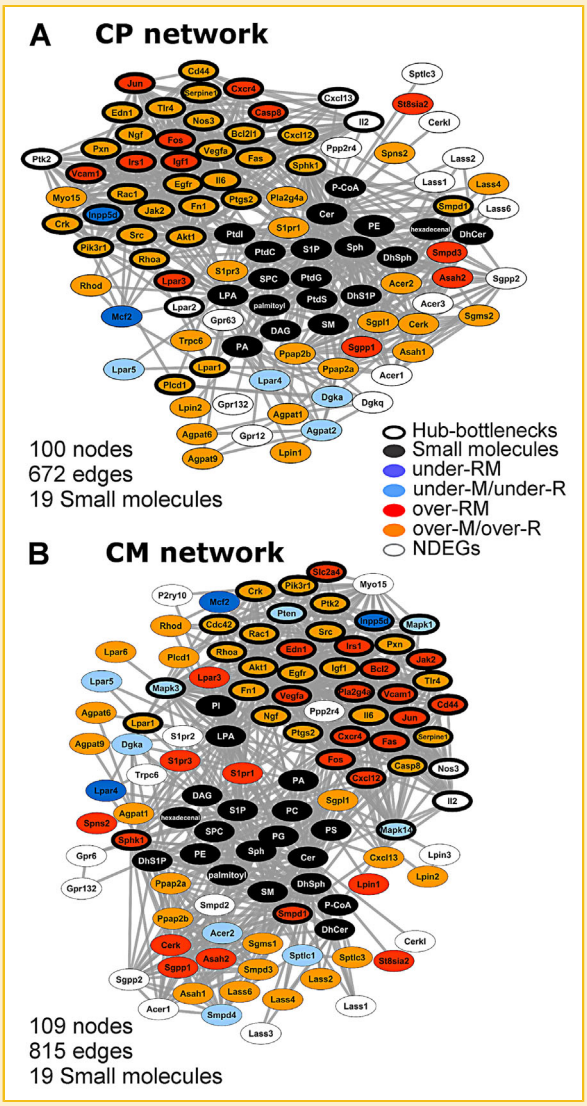

Fig. 3. (A) Subnetworks of the CP network represented by bioactive lipids and directly interacting nodes. (B) Subnetworks of the CM network represented by bioactive lipids and directly interacting nodes. The colored bars are described in the legend. Legend: thick edge, HB; black node, Small molecules; dark blue, underexpressed node-DEG based on both the RNA-seq and microarray analyses; light blue, underexpressed node-DEG based on either the RNA-seq or microarray analysis; red, overexpressed node-DEG based on both the RNA-seq and microarray analyses; orange, overexpressed node-DEG based on either the RNA-seq or microarray analysis; and white, non-DEG.

cell polarity, and adhesion during migration (Fig. 5B), as demonstrated by our GO analysis of the clusters and the overexpressed HBs (Fig. 4A, Supp. 3A–C, 4A and C) [Westhoff et al., 2004; Rathor et al., 2014]. In addition, the HB Pxn was an overexpressed node-DEG that is essential for focal adhesion complexes that interacted directly with LPA in the interactomic networks (Fig. 3). LPA was previously reported to stimulate Ptk2 and Pxn phosphorylation in a surface receptor-dependent manner, and this stimulation was shown to be essential for migration (Fig. 5B) [Liao et al., 2013].

Furthermore, cell motility and cell–cell contacts are related to filamin A (Flna), whose node-DEG was overexpressed in the CP and CM networks. Flna promotes cross-linking between plasma membrane Sphk1 and S1PR1, forming an intracellular signaling scaffold that is able to recruit Rho GTPases and orchestrate cell migration and lamellipodia formation (Fig. 5C) [Zhou et al., 2007; Maceyka et al., 2008]. Additionally, the PI3k/Akt pathway, which may be regulated by Cer and S1PR1, is required for the expression of cardiac transcription factors in mesodermal cells and has been associated with cardiac commitment, lamellipodia formation, and cytoskeletal reorganization via Rac1 activation [Faustino et al., 2008; Putnam et al., 2009; Castellano and Downward, 2011; Sheehy et al., 2012].

HEART DEVELOPMENT AND ECM REMODELING

Stable membrane rafts, which are enriched in cholesterol and SM, have been postulated to be necessary for the activity of hyaluronan synthase (Has). In the CP and CM networks, Has2 was an overexpressed node-DEG associated with Cd44, a hyaluronan receptor that interacts with Cer, as shown in Figure 3. In addition, Cer virtual knockout interfered with the betweenness value of Cd44 (Table II). Hyaluronan is an abundant component of cardiac jelly and is essential for the morphogenesis of the endocardial cushion and atrioventricular canal during heart development [Camenisch et al., 2001]. Furthermore, PI3K/Akt activation is associated with increased hyaluronan synthesis via a mechanism that involves S1P stimulation (Fig. 5D) [Qin et al., 2012].

According to the interference results, Cer and LPA virtual knockouts negatively affected Edn1 betweenness, indicating that these lipids can be important to Edn1 activity (Table II). Notably, Edn1, a peptide whose receptor (the endothelin B receptor, Ednrb) is associated with Cav1 in caveolae, is capable of increasing Cer and glycosphingolipid levels (Fig. 5B) [Catalán et al., 1996; Yamaguchi et al., 2003]. In addition, LPA has been observed to upregulate Edn1 in mouse embryonic fibroblasts [Stortelers et al., 2008]. The HBs Edn1 and Cav1 were overexpressed in the CP and CM networks, and Edn1 directly interacts with bioactive lipids in both networks (Fig. 3). Edn1 induces Nkx2.5 recruitment in cardiac progenitor cells and promotes the differentiation of pacemaker cells during cardiogenesis (Fig. 5B) [Zhang et al., 2012]. Furthermore, Edn1, S1P, and LPA are able to stimulate the expression of *Cyr61*, a gene whose protein is associated with extracellular matrix, cell adhesion, and migration through the binding of different integrins and is overexpressed in both the CP and CM networks [Mo and Lau, 2006]. However, *Cyr61*$^{-}$/$^{-}$ mice showed defects in valvuloseptal morphogenesis, inducing precocious apoptosis in cushion tissue, which can disrupt the fusion event [Mo and Lau, 2006].

Moreover, S1P promotes the nuclear accumulation of myocardin (Myocd), which was overexpressed in the CP and CM networks. Myocd transcriptionally co-activates Srf in a RhoA-dependent manner (Fig. 5D) [Zhao et al., 2014]. S1P and LPA activate Srf, which has been reported to regulate cardiac and smooth muscle genes, and the Srf-null mutant exhibits abnormal gastrulation and mesoderm development (Fig. 5D) [Brand, 2003; Lockman et al., 2004]. In addition, Srf activation by S1P and LPA is mediated by RhoA/Rho activity; GO analysis revealed Rho guanine-nucleotide exchange factor activity in the III-CP clusters (Supp. 3C).

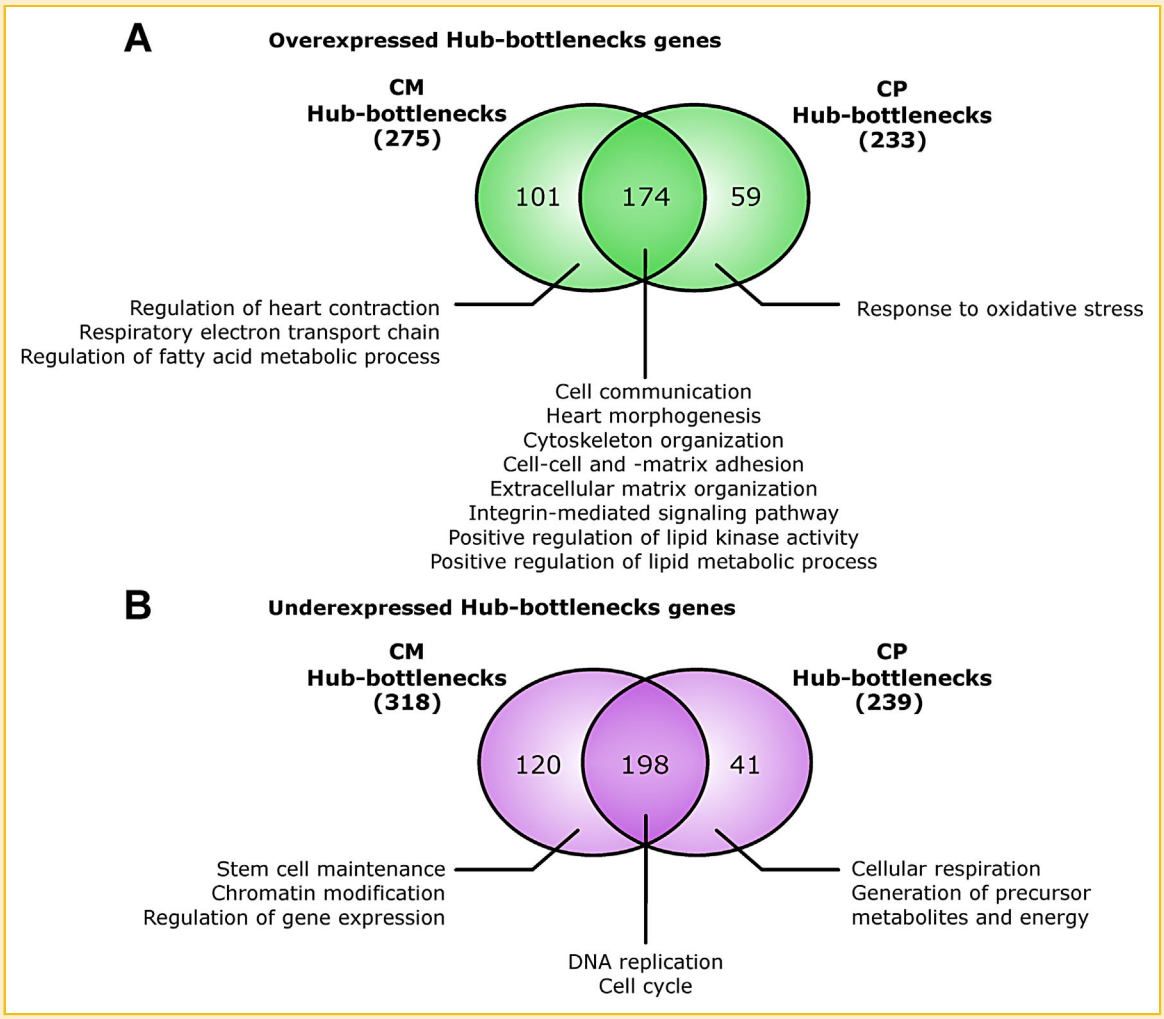

Fig. 4. (A) Comparative GO analysis of the overexpressed HB genes in the CM and CP networks. (B) Comparative GO analysis of the HBs that were underexpressed node-DEGs in the CM and CP networks.

In the CP and CM networks, Yap1 was an overexpressed node-DEG. The nuclear localization and activation of Yap1 are regulated by S1P via F-actin polymerization and Rho GTPase activation (Fig. 5D) [Miller et al., 2012]. Yap1 is considered a sensor and a mediator of the mechanotransduction that has been associated with cardiac regeneration and cardiac growth (Fig. 5D) [Xin et al., 2013]. Furthermore, Yap1 acts as a cofactor of Tbx5 (Fig. 5D), a transcription factor that is expressed in the heart tube during cardiac morphogenesis, and the loss of Tbx5 function causes heart septum defects [Horb and Thomsen, 1999].

In the CI–CP network, S1P virtual knockout interfered negatively with Nos3 (Table II). Nos3 was an overexpressed HB in the CP and CM networks that interacted directly with bioactive lipids, as shown in Figure 3. Furthermore, Nos3 deficiency results in congenital septal defects and heart failure via increased apoptosis in atrioventricular cushion regions, as well as increased incidence of bicuspid aortic valve formation [Liu and Feng, 2012].

Cardiac morphogenesis is an adhesion-dependent process in which integrin signaling mediates the interaction between the cell and the ECM, as well as cell–cell interactions [MacKenna et al., 2000]. Furthermore, integrin signaling activation is positively regulated by lipid rafts [Leitinger and Hogg, 2002]. Accordingly, integrin signaling and integrin binding were detected in the I-CP, II-CP, III-CP, and III-CM clusters (Supp. 3A–C and 4C), whereas ECM organization and ECM structural constituent were detected in I-CP, II-CP, III-CP, I-CM, and III-CM (Supp. 3A–C, 4A and C).

Interestingly, sphingolipids are co-regulators of the TGF-β signaling pathway, and cells transfected with sphingosine-1-phosphate phosphatase (Sgppl) show increased collagen type 1 alpha expression synergistically with the TGF-β cascade [Sato et al., 2003]. TGF-β1 was as an overexpressed HB found in both the CP and CM networks (Supp. 1). Furthermore, S1P transactivates the TGF-β receptor, thereby inducing Ctgf via Smad activation [Garrett et al., 2004; Katsuma et al., 2005]. Ctgf is also an overexpressed HB found in the CP and CM networks and has been associated with myofibroblast differentiation and collagen matrix contraction in response to mechanical activation [Garrett et al., 2004; Katsuma et al., 2005].

TABLE II. Most Relevant Virtual Knockouts of the HB Bioactive Lipids and Their Targets

Cluster	Virtual knockout	Target	Interference value	Description
Cluster I-CP	Cer	Serpine1	0.04	Serpin peptidase inhibitor, clade E
		Casp8	0.034	Caspase 8, apoptosis-related cysteine peptidase
		Cd44	0.032	CD44 antigen
		Ptgs2	0.022	Prostaglandin-endoperoxide synthase 2
		Fas	0.009	Fas cell surface death receptor
		Mmp9	−0.004	Matrix metallopeptidase 9
		Mmp2	−0.005	Matrix metallopeptidase 2
Cluster II-CP	Cer	Cd44	0.018	CD44 antigen
		Casp8	0.013	Caspase 8, apoptosis-related cysteine peptidase
		Serpine1	0.011	Serpin peptidase inhibitor, clade E
		Ptgs2	0.005	Prostaglandin-endoperoxide synthase 2
		Bcl2l1	0.002	BCL2-like 1
		Fas	0.002	Fas cell surface death receptor
		Il6	0.002	Interleukin 6
		Mmp9	−0.002	Matrix metallopeptidase 9
		Sphk1	−0.003	Sphingosine kinase 1
		Mmp2	−0.006	Matrix metallopeptidase 2
		Nos3	−0.014	Nitric oxide synthase 3
	S1P	Vegfa	0.014	Vascular endothelial growth factor A
		Nos3	0.007	Nitric oxide synthase 3
		Il6	0.006	Interleukin 6
		Ptgs2	0.005	Prostaglandin-endoperoxide synthase 2
		Rhoa	0.003	Ras homolog family member A
		Cxcl12	0.002	Chemokine (C-X-C motif) ligand 12
		Cxcr4	0.002	Chemokine (C-X-C motif) receptor 4
		Cxcl13	0.001	Chemokine (C-X-C motif) ligand 13
Cluster III-CP	PA	Mmp9	−0.004	Matrix metallopeptidase 9
	Cer	Ptgs2	0.071	Prostaglandin-endoperoxide synthase 2
		Fas	0.056	Fas cell surface death receptor
		Bcl2l1	0.038	BCL2-like 1
		Hand2	0.014	Heart and neural crest derivatives expressed transcript 2
		Edn1	0.005	Endothelin 1
		Lpar3	−0.004	Lysophosphatidic acid receptor 3
		S1pr1	−0.004	Sphingosine-1-phosphate receptor 1
	Sph	Cxcl12	−0.004	Chemokine (C-X-C motif) ligand 12
		Cxcr4	−0.005	Chemokine (C-X-C motif) receptor 4
		Src	−0.065	v-src avian sarcoma (Schmidt-Ruppin A-2) viral oncogene homolog
	LPA	Edn1	0.088	Endothelin 1
		Src	0.058	v-src avian sarcoma (Schmidt-Ruppin A-2) viral oncogene homolog
		Ptk2	0.054	Protein tyrosine kinase 2
		Pxn	0.037	Paxillin
		Egfr	0.01	Epidermal growth factor receptor
		Rhoa	−0.076	Ras homolog family member A
Cluster III-CM	Sph	Egfr	0.049	Epidermal growth factor receptor
		Src	−0.006	v-src avian sarcoma (Schmidt-Ruppin A-2) viral oncogene homolog
	LPA	Egfr	0.017	Epidermal growth factor receptor
		Edn1	0.015	Endothelin 1
		Ptk2	0.012	Protein tyrosine kinase 2
		Src	0.012	v-src avian sarcoma (Schmidt-Ruppin A-2) viral oncogene homolog
		Pxn	0.008	Paxillin
		Lpar3	0.007	Lysophosphatidic acid receptor 3
		Rhod	0.006	Ras homolog family member D

Moreover, S1P initiates a signaling cascade via S1PR1 and activates the transcription factor Stat3, which is necessary for energy production and heart remodeling, regulating gene expression associated with hypertrophic growth, development, and regeneration [Haghikia et al., 2014; Nguyen et al., 2014]. In the CP and CM networks, Stat3 appeared as an overexpressed HB and is able to impact ECM composition, regulating the expression of cytokines and genes associated with ECM, such as collagen [Haghikia et al., 2014]. Alterations to ECM homeostasis can lead to the loss of ECM components, promoting functional impairment and dilatation, or can induce the excess synthesis and deposition of ECM components, triggering enhanced fibrosis [Haghikia et al., 2014]. However, despite Stat3 promoting ECM component synthesis, Stat3-KO mice display increased expression of genes involved in fibrosis, such as Ctgf, Tnc, Serpine1, Thbs1, and Timp1, indicating that Stat3 modulates gene expression to maintain ECM homeostasis and acts as the most important molecule in communications between fibroblast and cardiomyocytes [Haghikia et al., 2014].

Furthermore, LPA activates and increases Mmp2 and Mmp9 gene expression in an LPA-receptor-signaling-dependent manner [Park et al., 2011; Kato et al., 2012; Komachi et al., 2012], promoting ECM degradation during cardiac loop formation and tissue remodeling (Fig. 5D), as detected in the I-CP, II-CP, and III-CM clusters (Supp. 3A, B and 4C), including metallopeptidase activity performed by Mmp2 and Mmp9 in III-CP (Supp. 3C) [Linask et al., 2005; Kim et al., 2011]. Furthermore, S1P is able to induce Timp2 cell release (Fig. 5D), which is required to generate active Mmp2, which was an overexpressed HB in both the CP and CM networks [Linask et al., 2005; Mascall et al., 2012]. In the interference results, Cer and PA virtual knockouts were observed to positively affect Mmp9 and Mmp2 betweenness, which

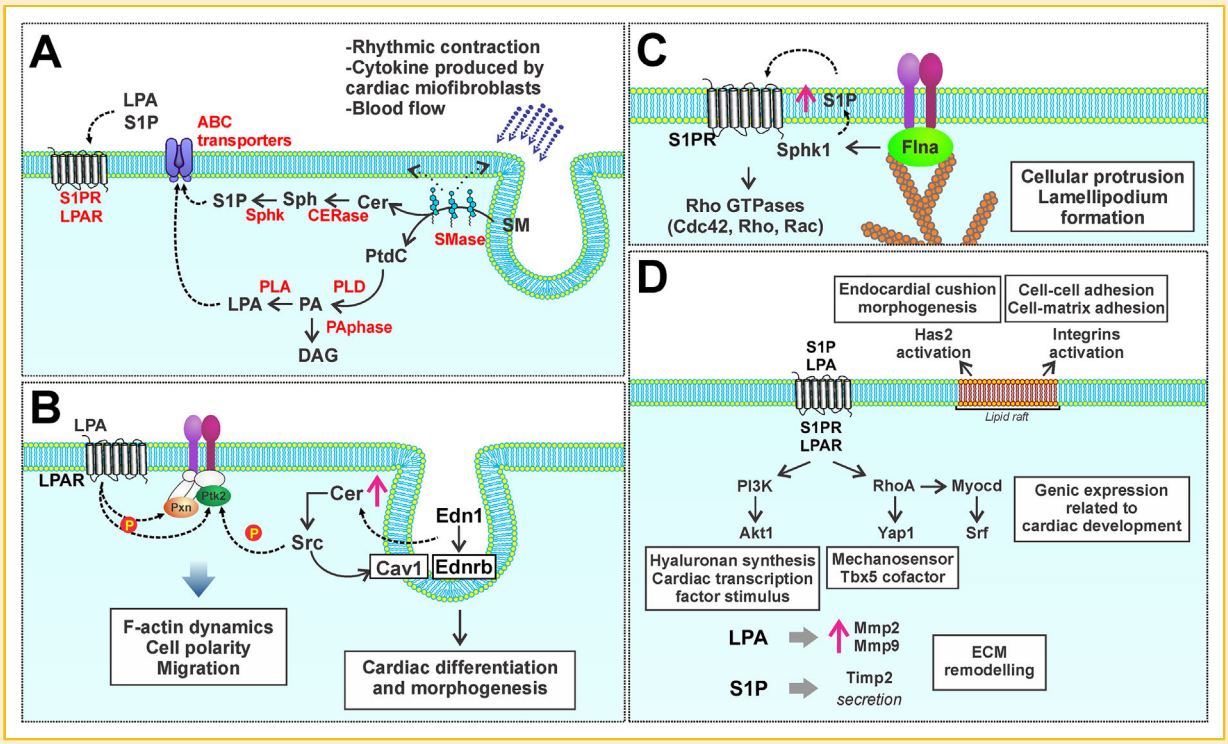

Fig. 5. (A) The plasma membrane is rich in caveolae that act as sensors of mechanical stimuli, which can be derived from cell contraction and blood flow that starts in E8 mice. These stimuli, along with the release of cytokines such as TNF-alpha and IL-6 by fibroblasts, transiently activate SMase, which converts SM to Cer and PtdC. Sph can be phosphorylated by SphK1, thereby forming S1P and avoiding the accumulation of Cer in the cell. However, PtdC can form PA through PLD activity, which is converted to DAG or LPA. In this sense, LPA and S1P can act intracellularly or be exported into the extracellular environment, where they act on specific receptors. (B) Cer is able to activate Src, which regulates the location of Cav1 in caveolae and is associated with Edrnb receptor-increased Cer, leading to cardiac differentiation and morphogenesis. In addition, Src mediates a phosphorylation of Ptk2, which promotes Ptk2 activation with the complex involving integrin. LPA can similarly induce the activation of Pxn and Ptk2, thereby promoting the dynamic modulation of F-actin and focal adhesions during migration, as well influencing cell polarity. (C) Furthermore, Flna interacts with the linking of actin filaments to the membrane by integrin and promotes crosslinking between SphK1 and S1PR in the plasma membrane, thereby increasing the localized synthesis of S1P and its associated receptor signaling. This mechanism triggers the activation of Rho GTPases, which are essential for cell protrusion and lamellipodium formation during migration. (D) Lipid rafts are essential for the activation of integrins, which can occur via PKC activation by S1P, and are associated with the activation of Has2. Furthermore, S1P and LPA can act via receptors to promote the activation of the PI3K/AKT signaling pathway, which induces the synthesis of hyaluronan by activating Has and promoting the expression of key transcription factors involved in cardiac development. Additionally, S1P induces Myocd translocation to and accumulation in the nucleus through the activation of Rho, which acts as a cofactor for Srf, thereby promoting the expression of genes essential to cardiogenesis. S1P also regulates the location of Yap1 through RhoA activation. Yap1 acts as a sensor and mediator of mechanotransduction, being associated with cardiac growth, in addition to acting as a cofactor for Tbx5, a cell cardiac marker. LPA can also stimulate the expression of Mmp2 and Mmp9, in addition to the regular S1P-mediated secretion of Timp2, which is associated with extracellular matrix remodeling and is essential for tissue remodeling and cardiac looping.

was expected, given that LPA and S1P positively regulate Mmp9 and Mmp2, and the presence of these lipids is associated with Cer and PA conversion.

Serpine1 was an overexpressed HB, whose betweenness topology was negatively affected by Cer virtual knockout (Table II). Interestingly, SMases and Cer induce Serpine1 release in response to Tnf-α stimulation in vascular endothelial cells [Soeda et al., 1995; Soeda et al., 1998]. Serpine1 is also involved in cardiac remodeling and the regulation of cell adhesion and migration, in addition to influencing ECM homeostasis [Xu et al., 2010; Czekay et al., 2011].

INFLAMMATORY AND APOPTOTIC MOLECULES ASSOCIATED WITH BIOACTIVE LIPID SIGNALING

According to our interference analysis, Cer virtual knockout negatively affected the betweenness score of Casp8, Fas, and Bcl2l1 in the CI-CP, CII-CP, and CIII- CP networks, indicating that Cer signaling can play a role in the activity of these gene products (Table II). In the CP network, Casp8, Fas, and Bcl2l1 were overexpressed HB node-DEGs that directly interacted with Cer, while in the CM network, Cer interacted with Casp8 and Bcl2 (Fig. 3). This lipid is associated with apoptosis induction, being activated by Fas, leading the mitochondrial Ca^{2+} increase and activating Casp and Bid [Darios et al., 2003]. Apoptosis is an essential mechanism during embryogenesis that orchestrates tissue morphogenesis during development by eliminating unwanted cells and was represented by GO analysis in the CI-CP, CIII-CP, and CIII-CM networks (Supp. 3A, C and 4C) [Sakamaki et al., 2002]. Casp8-null mice were previously shown to die at E11.5, presenting neural and cardiac formation defects [Sakamaki et al., 2002]. In addition, Cer affects Bcl2 function by inducing the dephosphorylation of serine 70, whose

phosphorylation is necessary for the anti-apoptotic activity of Bcl2 [Ruvolo et al., 1999].

Furthermore, S1P virtual knockout affected the betweenness scores of Il6, Cxcl12, Cxcl13, and Cxcr4 in CII-CP (Table II). Il6 was an overexpressed HB node-DEG in the CP and CM networks that interacted directly with S1P. This cytokine is secreted by cardiofibroblasts and functions in heart remodeling [Porter and Turner, 2009]. Cardiac cells that lack Il6 activity attenuated the activation of Stat3 and Vegfa production, leading to interstitial collagen accumulation, which promotes cardiac dilatation and ventricular dysfunction [Banerjee et al., 2009; Porter and Turner, 2009]. In both the CP and CM networks, Cxcr4, Cxcl12, and Cxcl13 interacted directly with S1P (Fig. 3). S1P has been shown to cooperate with Cxcl12 to increase cell adhesion in an $\alpha 4\beta 1$ integrin-dependent manner [García-Bernal et al., 2013]. In addition, Cxcl12 can drive neural crest cell migration and bind to its main receptor Cxcr7, which heterodimerizes with Cxcr4 and potentiate Cxcl12 responses [Escot et al., 2013]. Neural crest cells in *Cxcl12*$^{-/-}$ or *Cxcr4*$^{-/-}$ mice showed delayed migration and increased apoptosis, which leads to malformation of the conotroncus region, ventricular septum defects, and double-outlet right ventricle [Escot et al., 2013]. Moreover, in stromal cells and hematopoietic progenitors, S1P was observed to induce Cxcl12 release [Golan et al., 2012].

In the CI-CP, CII-CP, and CIII-CP networks, Ptgs2 betweenness score was negatively affected by the virtual knockout of S1P and Cer (Table II). In both the CP and CM networks, Ptgs2 directly interacts with Cer and S1P (Fig. 3) and is essential for proper myocardial cell morphogenesis in the atrioventricular valve region [Scherz et al., 2008]. Different studies observed that S1P induces *Ptgs2* expression and the promotion of prostaglandin e2 release in response to TNF-α, which is secreted by cardiofibroblasts [Pettus et al., 2003; Porter and Turner, 2009; Hsu et al., 2015]. In addition, Egfr activation is also associated with increased *Ptgs2* expression (Xu and Shu, 2007). However, given that Egfr is located in lipid rafts and that transactivation is regulated by S1P, this lipid may be related to *Ptgs2* expression mediated by Egfr [Tanimoto et al., 2004]. Egfr acts in valve formation during cardiac development by modulating the activity of Pld2 and Bmp, as well as by interacting with Sph and LPA. Egfr is also negatively affected by the virtual knockout of these lipids [Czarny et al., 2000; Iwamoto and Mekada, 2006].

CONCLUSIONS

In this study, we propose an interaction between the extracellular environment, which is composed of matrix molecules, and bioactive signaling lipids. External environmental stimuli and morphogens affect lipid membrane composition and lipid rafts, inducing several signaling cascades by altering the levels of available Cer, SM, and cholesterol. Additionally, transient changes in the Cer and SM levels can stimulate S1P and LPA and activate signaling cascades associated with cell communication, adhesion, and motility. The signaling pathways modulated by bioactive lipids also induce the remodeling of the ECM and the synthesis of new ECM components. Currently, it is understood that changes in the external cellular environment can regulate gene expression. Similarly, this study suggests that the signaling activated by bioactive lipids may be associated with the cellular response to various stimuli; these responses generate cell signaling and gene expression adaptation during differentiation and cardiac morphogenesis.

ACKNOWLEDGMENTS

This work was supported by the Conselho Nacional de Desenvolvimento Científico e Tecnológico (CNPq) through grant 301149/2012-7, Coordenação de Aperfeiçoamento de Pessoal de Nível Superior (CAPES) through grant 004/12 and Fundação de Amparo à Pesquisa do Rio Grande do Sul (Fapergs) through grant 11/2072-2. We also thank Msc. Bruno César Feltes for critically reading the manuscript, Dr. Giovanni Scardoni for aiding in the interference analysis and Msc. Kendi Nishino Miyamoto for helping with the transcriptomic microarray analysis.

REFERENCES

Anders S, Pyl PT, Huber W. 2014. HTSeq: A python framework to work with high- throughput sequencing data. Bioinformatics 31:166–169.

Armstrong D, Zidovetzki R. 2008. Amplification of diacylglycerol activation of protein kinase C by cholesterol. Biophys J 94:4700–4710.

Bader GD, Hogue CWV. 2003. An automated method for finding molecular complexes in large protein interaction networks. BMC Bioinformatics 4:2.

Banerjee I, Fuseler JW, Intwala AR, Baudino TA. 2009. IL-6 loss causes ventricular dysfunction, fibrosis, reduced capillary density, and dramatically alters the cell populations of the developing and adult heart. Am J Physiol Heart Circ Physiol 296:H1694–H1704.

Benjamini Y, Hochberg Y. 1995. Controlling the false discovery rate: A practical and powerful approach to multiple. J Royal Stat Soc Ser B (Methodol) 57:289–300.

Berdichevets IN, Tyazhelova T V, Shimshilashvili KR, Rogaev EI. 2010. Lysophosphatidic acid is a lipid mediator with wide range of biological activities. Biosynthetic pathways and mechanism of action. Biochemistry. Biokhimii⌢a 75:1088–1097.

Bieberich E. 2012. It′s a lipid′s world: Bioactive lipid metabolism and signaling in neural stem cell differentiation. Neurochem Res 37:1208–1229.

Bowers SLK, Banerjee I, Baudino TA. 2010. The extracellular matrix: At the center of it all. J Mol Cell Cardiol 48:474–482.

Brand T. 2003. Heart development: Molecular insights into cardiac specification and early morphogenesis. Dev Biol 258:1–19.

Camenisch TD, Biesterfeldt J, Brehm-Gibson T, Bradley J, McDonald J. 2001. Regulation of cardiac cushion development by hyaluronan. Exp Clin Cardiol 6:4–10.

Carbon S, Ireland A, Mungall CJ, Shu S, Marshall B, Lewis S, AmiGO Hub & Web Presence Working Group 2009. 2009. AmiGO: Online access to ontology and annotation data. Bioinformatics. (Oxford, England) 25:288–289.

Castellano E, Downward J. 2011. RAS interaction with PI3K: More than just another effector pathway. Genes Cancer 2:261–274.

Catalán RE, Aragonés MD, Martínez AM, Fernández I. 1996. Involvement of sphingolipids in the endothelin-1 signal transduction mechanism in rat brain. Neurosci Lett 220:121–124.

Chen J-N, Cowan DB, Mably JD. 2005. Cardiogenesis and the regulation of cardiac- specific gene expression. Heart Fail Clin 1:157–170.

Cline MS, Smoot M, Cerami E, Kuchinsky A, Landys N, Workman C, Christmas R, Avila-Campilo I, Creech M, Gross B, Hanspers K, Isserlin R, Kelley R, Killcoyne S, Lotia S, Maere S, Morris J, Ono K, Pavlovic V, Pico AR, Vailaya A,

Wang PL, Adler A, Conklin BR, Hood L, Kuiper M, Sander C, Schmulevich I, Schwikowski B, Warner GJ, Ideker T, Bader GD. 2007. Integration of biological networks and gene expression data using Cytoscape. Nat Protoc 2:2366–2382.

Czarny M, Fiucci G, Lavie Y, Banno Y, Nozawa Y, Liscovitch M. 2000. Phospholipase D2: Functional interaction with caveolin in low-density membrane microdomains. FEBS Lett 467:326–332.

Czarny M, Schnitzer JE. 2004. Neutral sphingomyelinase inhibitor scyphostatin prevents and ceramide mimics mechanotransduction in vascular endothelium. Am J Physiol Heart Circ Physiol 287: H1344–H1352.

Czekay R-P, Wilkins-Port CE, Higgins SP, Freytag J, Overstreet JM, Klein RM, Higgins CE, Samarakoon R, Higgins PJ. 2011. PAI-1: An integrator of cell signaling and migration. Int J Cell Biol 2011:562481.

Darios F, Lambeng N, Troadec J-D, Michel PP, Ruberg M. 2003. Ceramide increases mitochondrial free calcium levels via caspase 8 and Bid: Role in initiation of cell death. J Neurochem 84:643–654.

Escot S, Blavet C, Härtle S, Duband J-L, Fournier-Thibault C. 2013. Misregulation of SDF1-CXCR4 signaling impairs early cardiac neural crest cell migration leading to conotruncal defects. Circ Res 113:505–516.

Fahy E, Sud M, Cotter D, Subramaniam S. 2007. LIPID MAPS online tools for lipid research. Nucleic Acids Res 35:W606–W612.

De Faria Poloni J, Chapola H, Feltes BC, Bonatto D. 2014. The importance of sphingolipids and reactive oxygen species in cardiovascular development. Biol Cell. 106:167–181.

Faustino RS, Behfar A, Perez-Terzic C, Terzic A. 2008. Genomic chart guiding embryonic stem cell cardiopoiesis. Genome Biol 9:R6.

Feltes BC, Bonatto D. 2013. Combining small molecules for cell reprogramming through an interatomic analysis. Mol Biosyst 9:2741–2763.

Franceschini A, Szklarczyk D, Frankild S, Kuhn M, Simonovic M, Roth A, Lin J, Minguez P, Bork P, von Mering C, Jensen LJ. 2013. STRING v9.1: Protein-protein interaction networks, with increased coverage and integration. Nucleic Acids Res 41:D808–D815.

García-Bernal D, Redondo-Muñoz J, Dios-Esponera A, Chèvre R, Bailón E, Garayoa M, Arellano-Sánchez N, Gutierrez NC, Hidalgo A, García-Pardo A, Teixidó J. 2013. Sphingosine-1-phosphate activates chemokine-promoted myeloma cell adhesion and migration involving α4β1 integrin. J Pathol 229:36–48.

Garrett Q, Khaw PT, Blalock TD, Schultz GS, Grotendorst GR, Daniels JT. 2004. Involvement of CTGF in TGF-B1-stimulation of myofibroblast differentiation and collagen matrix contraction in the presence of mechanical stress. Invest Ophthalmol Vis Sci 45:1109–1116.

Golan K, Vagima Y, Ludin A, Itkin T, Cohen-Gur S, Kalinkovich A, Kollet O, Kim C, Schajnovitz A, Ovadya Y, Lapid K, Shivtiel S, Morris AJ, Ratajczak MZ, Lapidot T. 2012. S1P promotes murine progenitor cell egress and mobilization via S1P1-mediated ROS signaling and SDF-1 release. Blood 119:2478–2488.

Granados-Riveron JT, Brook JD. 2012. Formation, contraction, and mechanotransduction of myofribrils in cardiac development: Clues from genetics. Biochem Res Int 2012:504906.

Groenendijk BCW, Van der Heiden K, Hierck BP, Poelmann RE. 2007. The role of shear stress on ET-1, KLF2, and NOS-3 expression in the developing cardiovascular system of chicken embryos in a venous ligation model. Physiology (Bethesda. Md.) 22:380–389.

Haghikia A, Ricke-Hoch M, Stapel B, Gorst I, Hilfiker-Kleiner D. 2014. STAT3, a key regulator of cell-to-cell communication in the heart. Cardiovasc Res 102:281–289.

Hannun YA, Obeid LM. 2008. Principles of bioactive lipid signalling: Lessons from sphingolipids. Nat Rev Mol Cell Biol 9:139–150.

Horb ME, Thomsen GH. 1999. Tbx5 is essential for heart development. Development (Cambridge. England) 126:1739–1751.

Hsu CK, Lee IT, Lin CC, Hsiao LD, Yang CM. 2015. Sphingosine-1-phosphate mediates COX-2 expression and PGE2 /IL-6 secretion via c-Src-dependent AP-1 activation. J Cell Physiol 230:702–715.

Iwamoto R, Mekada E. 2006. ErbB and HB-EGF signaling in heart development and function. Cell Struct Funct 31:1–14.

Kanehisa M, Goto S. 2000. KEGG: Kyoto encyclopedia of genes and genomes. Nucleic Acids Res 28:27–30.

Karliner JS, Honbo N, Summers K, Gray MO, Goetzl EJ. 2001. The lysophospholipids sphingosine-1-phosphate and lysophosphatidic acid enhance survival during hypoxia in neonatal rat cardiac myocytes. J Mol Cell Cardiol 33:1713–1717.

Kato K, Fukui R, Okabe K, Tanabe E, Kitayoshi M, Fukushima N, Tsujiuchi T. 2012. Constitutively active lysophosphatidic acid receptor-1 enhances the induction of matrix metalloproteinase-2. Biochem Biophys Res Commun 417:790–793.

Katsuma S, Ruike Y, Yano T, Kimura M, Hirasawa A, Tsujimoto G. 2005. Transcriptional regulation of connective tissue growth factor by sphingosine 1 -phosphate in rat cultured mesangial cells. FEBS Lett 579:2576–2582.

Kim E-S, Kim J-S, Kim SG, Hwang S, Lee CH, Moon A. 2011. Sphingosine 1-phosphate regulates matrix metalloproteinase-9 expression and breast cell invasion through S1P3-Gαq coupling. J Cell Sci 124:2220–2230.

Kleger A, Liebau S, Lin Q, von Wichert G, Seufferlein T. 2011. The impact of bioactive lipids on cardiovascular development. Stem Cells Int 2011:916180.

Komachi M, Sato K, Tobo M, Mogi C, Yamada T, Ohta H, Tomura H, Kimura T, Im D-S, Yanagida K, Ishii S, Takeyoshi I, Okajima F. 2012. Orally active lysophosphatidic acid receptor antagonist attenuates pancreatic cancer invasion and metastasis in vivo. Cancer Science 103:1099–1104.

Kuhn M, Szklarczyk D, Franceschini A, von Mering C, Jensen LJ, Bork P. 2012. STITCH 3: zooming in on protein-chemical interactions. Nucleic Acids Res 40:D876–D880.

Kupperman E, An S, Osborne N, Waldron S, Stainier DYR. 2000. A sphingosine-1-phosphate receptor regulates cell migration during vertebrate heart development. Nature 406:192–195.

Langmead B, Salzberg SL. 2012. Fast gapped-read alignment with Bowtie 2. Nat Methods 9:357–359.

Leitinger B, Hogg N. 2002. The involvement of lipid rafts in the regulation of integrin function. J Cell Sci 115:963–972.

Liao Y, Mu G, Zhang L, Zhou W, Zhang J, Yu H. 2013. Lysophosphatidic acid stimulates activation of focal adhesion kinase and paxillin and promotes cell motility, via LPA1-3, in human pancreatic cancer. Dig Dis Sci 58:3524–3533.

Linask KK, Han M, Cai DH, Brauer PR, Maisastry SM. 2005. Cardiac morphogenesis: Matrix metalloproteinase coordination of cellular mechanisms underlying heart tube formation and directionality of looping. Dev Dyn 233:739–753.

Little CD, Rongish BJ. 1995. The extracellular matrix during heart development. Experientia 51:873–882.

Liu Y, Feng Q. 2012. NOing the heart: Role of nitric oxide synthase-3 in heart development. Differentiation 84:54–61.

Lockman K, Hinson JS, Medlin MD, Morris D, Taylor JM, Mack CP. 2004. Sphingosine 1-phosphate stimulates smooth muscle cell differentiation and proliferation by activating separate serum response factor co- factors. J Biol Chem 279:42422–42430.

Maceyka M, Alvarez SE, Milstien S, Spiegel S. 2008. Filamin A links sphingosine kinase 1 and sphingosine-1-phosphate receptor 1 at lamellipodia to orchestrate cell migration. Mol Cell Biol 28:5687–5697.

MacKenna D, Summerour SR, Villarreal FJ. 2000. Role of mechanical factors in modulating cardiac fibroblast function and extracellular matrix synthesis. Cardiovasc Res 46:257–263.

Maere S, Heymans K, Kuiper M. 2005. BiNGO: A Cytoscape plugin to assess overrepresentation of gene ontology categories in biological networks. Bioinformatics (Oxford. England) 21:3448–3449.

Mascall KS, Small GR, Gibson G, Nixon GF. 2012. Sphingosine-1-phosphate-induced release of TIMP-2 from vascular smooth muscle cells inhibits angiogenesis. J Cell Sci 125:2267–2275.

Miller E, Yang J, DeRan M, Wu C, Su AI, Bonamy GMC, Liu J, Peters EC, Wu X. 2012. Identification of serum-derived sphingosine- 1-phosphate as a small molecule regulator of YAP. Chem Biol 19:955–962.

Mo F-E, Lau LF. 2006. The matricellular protein CCN1 is essential for cardiac development. Circ Res 99:961–969.

Newman MEJ. 2005. A measure of betweenness centrality based on random walks. Social Networks 27:39–54.

Nguyen A V, Wu YY, Lin EY. 2014. STAT3 and sphingosine-1-phosphate in inflammation-associated colorectal cancer. World J Gastroenterol 20:10279–10287.

Park SY, Jeong KJ, Panupinthu N, Yu S, Lee J, Han JW, Kim JM, Lee JS, Kang J, Park CG, Mills GB, Lee HY. 2011. Lysophosphatidic acid augments human hepatocellular carcinoma cell invasion through LPA1 receptor and MMP-9 expression. Oncogene 30:1351–1359.

Patel RK, Jain M. 2012. NGS QC Toolkit: A toolkit for quality control of next generation sequencing data. PloS ONE 7:e30619.

Pettus BJ, Bielawski J, Porcelli, AM, Reames DL, Johnson KR, Morrow J, Chalfant CE, Obeid LM, Hannun YA. 2003. The sphingosine kinase 1/sphingosine-1- phosphate pathway mediates COX-2 induction and PGE2 production in response to TNF-alpha. FASEB J 17:1411–1421.

Porter KE, Turner NA. 2009. Cardiac fibroblasts: At the heart of myocardial remodeling. Pharmacol Ther 123:255-278.

Putnam AJ, Schulz V V, Freiter EM, Bill HM, Miranti CK. 2009. Src, PKCalpha, and PKCdelta are required for alphavbeta3 integrin-mediated metastatic melanoma invasion. Cell Commun Signal 7:10.

Qin J, Berdyshev E, Poirer C, Schwartz NB, Dawson G. 2012. Neutral sphingomyelinase 2 deficiency increases hyaluronan synthesis by up-regulation of Hyaluronan synthase 2 through decreased ceramide production and activation of Akt. J Biol Chem 287:13620–13632.

Rathor N, Zhuang R, Wang J-Y, Donahue JM, Turner DJ, Rao JN. &2014. Src-mediated caveolin-1 phosphorylation regulates intestinal epithelial restitution by altering Ca(2+) influx after wounding. Am J Physiol Gastrointest Liver Physiol. 306:G650–G658.

Rivals I, Personnaz L, Taing L, Potier M-C. 2007. Enrichment or depletion of a GO category within a class of genes: Which test? Bioinformatics (Oxford. England) 23:401–407.

Robinson MD, McCarthy DJ, Smyth GK. 2010. EdgeR: A Bioconductor package for differential expression analysis of digital gene expression data. Bioinformatics (Oxford. England) 26:139–140.

Rozario T, Desimone DW. 2010. The extracellular matrix in development and morphogenesis: A dynamic view. Dev Biol 341:126–140.

Ruvolo PP, Deng X, Ito T, Carr BK, May WS. 1999. Ceramide iInduces Bcl2 dephosphorylation via a mechanism involving mitochondrial PP2A. J Biol Chem 274:20296–20300.

Sakamaki K, Inoue T, Asano M, Sudo K, Kazama H, Sakagami J, Sakata S, Ozaki M, Nakamura S, Toyokuni S, Osumi N, Iwakura Y, Yonehara S. 2002. Ex vivo whole-embryo culture of caspase-8-deficient embryos normalize their aberrant phenotypes in the developing neural tube and heart. Cell Death Differ 9:1196–1206.

Sato M, Markiewicz M, Yamanaka M, Bielawska A, Mao C, Obeid LM, Hannun YA, Trojanowska M. 2003. Modulation of transforming growth factor-beta (TGF-beta) signaling by endogenous sphingolipid mediators. J Biol Chem 278:9276–9282.

Scardoni G, Montresor A, Tosadori G, Laudanna C. 2014. Node interference and robustness: Performing virtual knock-out experiments on biological networks: The case of leukocyte integrin activation network. PloS ONE 9:e88938.

Scardoni G, Laudanna C. 2012. Centralities Based Analysis of Complex Networks. In: Zhang Y, editor. New Frontiers in Graph Theory. InTech. pp 323–348.

Scardoni G, Petterlini M, Laudanna C. 2009. Analyzing biological network parameters with CentiScaPe. Bioinformatics (Oxford. England) 25:2857–2859.

Scherz PJ, Huisken J, Sahai-Hernandez P, Stainier DYR. 2008. High- speed imaging of developing heart valves reveals interplay of morphogenesis and function. Development (Cambridge. England) 135:1179–1187.

Sheehy SP, Grosberg A, Parker KK. 2012. The contribution of cellular mechanotransduction to cardiomyocyte form and function. Biomech Model Mechanobiol 11:1227–1239.

Smoot ME, Ono K, Ruscheinski J, Wang P-L, Ideker T. 2011. Cytoscape 2.8: New features for data integration and network visualization. Bioinformatics (Oxford, England) 27:431–432.

Soeda S, Honda O, Shimeno H, Nagamatsu A. 1995. Sphingomyelinase and cell-permeable ceramide analogs increase the release of plasminogen activator inhibitor-1 from cultured endothelial cells. Thromb Res 80:509–518.

Soeda S, Tsunoda T, Kurokawa Y, Shimeno H. 1998. Tumor necrosis factor-alpha-induced release of plasminogen activator inhibitor-1 from human umbilical vein endothelial cells: Involvement of intracellular ceramide signaling event. Biochim Biophys Acta 1448:37–45.

Stortelers C, Kerkhoven R, Moolenaar WH. 2008. Multiple actions of lysophosphatidic acid on fibroblasts revealed by transcriptional profiling. BMC Genomics 9:387.

Tanimoto T, Lungu AO, Berk BC. 2004. Sphingosine 1-phosphate trans-activates the platelet-derived growth factor beta receptor and epidermal growth factor receptor in vascular smooth muscle cells. Circ Res 94:1050–1058.

Trapnell C, Roberts A, Goff L, Pertea G, Kim D, Kelley DR, Pimentel H, Salzberg SL, Rinn JL, Pachter L. 2012. Differential gene and transcript expression analysis of RNA-seq experiments with TopHat and Cufflinks. Nat Protoc 7:562–578.

Wamstad JA, Alexander JM, Truty RM, Shrikumar A, Li F, Eilertson KE, Ding H, Wylie JN, Pico AR, Capra A, Erwin G, Kattman SJ, Keller GM, Srivastava D, Levine SS, Pollard KS, Holloway AK, Boyer LA, Bruneau BG. 2012. Dynamic and coordinated epigenetic regulation of developmental transitions in the cardiac lineage. Cell 151:206–220.

Wang X, Devaiah SP, Zhang W, Welti R. 2006. Signaling functions of phosphatidic acid. Prog Lipid Res 45:250–278.

Wendler CC, Rivkees SA. 2006. Sphingosine-1-phosphate inhibits cell migration and endothelial to mesenchymal cell transformation during cardiac development. Dev Biol 291:264–277.

Westhoff MA, Serrels B, Fincham VJ, Frame MC, Carragher NO. 2004. Src-mediated phosphorylation of focal adhesion kinase couples actin and adhesion dynamics to survival signaling src-mediated phosphorylation of focal adhesion kinase couples actin and adhesion dynamics to survival signaling. Mol Cell Biol 24:8113–8133.

Wozniak MA, Chen CS. 2009. Mechanotransduction in development: A growing role for contractility. Nat Rev Mol Cell Biol 10:34–43.

Xin M, Kim Y, Sutherland LB, Murakami M, Qi X, McAnally J, Porrello ER, Mahmoud AI, Tan W, Shelton JM, Richardson J a, Sadek H a, Bassel-Duby R, Olson EN. 2013. Hippo pathway effector Yap promotes cardiac regeneration. Proc Natl Acad Sci U S A 110:13839–13844.

Xu K, Shu H-KG. 2007. EGFR activation results in enhanced cyclooxygenase-2 expression through p38 mitogen-activated protein kinase-dependent activation of the Sp1/Sp3 transcription factors in human gliomas. Cancer Res 67:6121–6129.

Xu YJ, Panagia V, Shao Q, Wang X, Dhalla NS. 1996. Phosphatidic acid increases intracellular free Ca2+ and cardiac contractile force. Am Physiol Soc 271:H651–H659.

Xu Z, Castellino FJ, Ploplis VA. 2010. Plasminogen activator inhibitor-1 (PAI-1) is cardioprotective in mice by maintaining microvascular integrity and cardiac architecture. Blood 115:2038–2047.

Yamaguchi T, Murata Y, Fujiyoshi Y, Doi T. 2003. Regulated interaction of endothelin B receptor with caveolin-1. Eur J Biochem 270:1816–1827.

Zhang X, Guo J-P, Chi Y-L, Liu Y-C, Zhang C-S, Yang X-Q, Lin H-Y, Jiang E-P, Xiong S-H, Zhang Z-Y, Liu B-H. 2012. Endothelin-induced differentiation of Nkx2.5^{+} cardiac progenitor cells into pacemaking cells. Mol Cell Biochem 366:309–318.

Zhao X, Ding EY, Yu OM, Xiang SY, Tan-Sah VP, Yung BS, Hedgpeth J, Neubig RR, Lau LF, Brown JH, Miyamoto S. 2014. Induction of the matricellular protein CCN1 through RhoA and MRTF-A contributes to ischemic cardioprotection. J Mol Cell Cardiol 75:152–161.

Zhou X, Borén J, Akyürek LM. 2007. Filamins in cardiovascular development. Trends Cardiovasc Med 17:222–229.

SUPPORTING INFORMATION

Additional Supporting Information may be found in the online version of this article.